

Raman spectral analysis of the brainstem and responses of neuroglia and cytokines in whole-body gamma-irradiated rats after administration of aminothioli-based radioprotector GL2011

Dušica M. Kočović^{1,*}, Danica Bajuk-Bogdanović², Irina Maslovarić³, Biljana Božić Nedeljković¹, Pavle R. Andjus¹ and Marko Daković²

¹Faculty of Biology, University of Belgrade, Studentski trg 3, Belgrade 11000, Serbia

²Faculty of Physical Chemistry, University of Belgrade, Studentski trg 12-16, Belgrade 11000, Serbia

³Institute for Medical Research, University of Belgrade, Dr Subotića 4, P.O.B. 39, 11129 Belgrade 102, Serbia

*Corresponding author: dusica.kocovic@bio.bg.ac.rs

Received: January 29, 2021; Revised: February 19, 2021; Accepted: February 22, 2021; Published online: February 26, 2021

Abstract: The search for an effective and non-toxic radioprotector is ongoing. We tested a novel, natural aminothioli-based radioprotector, GL2011, that was applied 30 min, 3 h or 6 h after the exposure of male albino Wistar rats to a 6.7 Gy mild dose of gamma radiation. The molecular signatures of radioprotection were investigated with Raman microspectroscopy of brainstem tissue samples. Morphological changes and activation of astrocytes and microglia were assessed by immunohistochemistry. Global markers of neuroinflammation were followed by ELISA to monitor blood plasma levels of pro-inflammatory (IL-6 and TNF- α) and anti-inflammatory (IL-10) cytokines. A thirty-day follow-up determined survival of unprotected animals 37.5%. A survival increase was observed after radioprotection (75%, irrespective of the time of application). Raman spectra revealed a slightly deleterious effect of radiation on nucleic acids in surviving animals that was mitigated with the radioprotector, as GL2011 preserved the morphology of both astrocytes and microglia, with reduced microglial infiltration. Cytokine assessment revealed an immunomodulatory effect of the novel radioprotector. The overall results point out the positive effects of a single dose of GL2011 applied at different times. The molecular and cellular changes in the brainstem indicate that the radioprotector applied after radiation conferred better protection, which underlines its translation to cure radiation accidents.

Keywords: rat brainstem; irradiation; aminothioli; radioprotector GL2011; Raman microspectroscopy; glial cell markers; cytokines

INTRODUCTION

In whole-body exposure to X- or gamma radiation (e.g. during radiation accidents) it is of particular interest to assess the damage to brain tissue and to determine efficient means of radioprotection. At the molecular and cellular levels, irradiation triggers a cascade of direct and indirect effects, including activation of early response transcription factors, signal transduction messengers, alterations of biomacromolecules and cellular effects particularly with regard to neuroglia [1,2]. From a biological perspective, the precise mechanisms of neurotoxicity and neurodegeneration following ionizing radiation exposure remain poorly

elucidated [3] and post-irradiation therapy remains underdeveloped [4].

Radioprotectors are substances designed to reduce mortality and the harmful effects of ionizing radiation. With regards to the potential application of ionizing radiation in external beam radiation therapy and in cases of accidental exposure to radiation, screening for radioprotective compounds is of great importance. Nevertheless, there is only one agent that has been approved by the Food and Drug Administration (USA) for use in cancer radiation treatment, and that is amifostine, (2-[(3-aminopropyl)amino]ethanethioli dihydrogen phosphate). *In vitro* and *in vivo* studies

have revealed the basis of its action in free radical-scavenging [5]. However, amifostine is effective only if administered immediately prior to irradiation, so its use is of limited value in a number of clinical indications and it is unsuitable for cases of incidental irradiation [6]. Moreover, it was found that amifostine produces side effects such as nausea, hypotension, vomiting, hypocalcemia and allergic reactions [7]. Thus, its application is limited, especially at the higher doses necessary to enable successful radioprotection, particularly in accidental radiation cases [8,9].

Among ongoing studies on both natural and synthetic radioprotective agents, aminothiols have shown some promising results [10-12]. Various mechanisms of action of these radioprotectors on cellular DNA have been proposed, such as free radical scavenging, induction of hypoxia, formation of mixed disulfides, and hydrogen and electron donation as mechanisms of free radical elimination leading to restoration of damaged cellular components [13,14]. This study is a continuation of a preclinical trial of the radioprotective effects of a newly synthesized, naturally occurring aminothiol compound, GL2011 [15,16] that acts as an antioxidant and immunostimulatory agent. Its non-toxicity to albino Wistar rats was also confirmed. After intraperitoneal application in three identical doses (100 mg/kg b.w.) at three time points (30 min prior to irradiation, 3 h and 6 h after irradiation), GL2011 significantly reduced the mortality of whole-body irradiated animals (87% survival compared to 30% survival of unprotected animals [15]). GL2011 was shown to have a significant effect on the regeneration of intestinal epithelial microvilli [15] and bone marrow cells of irradiated animals 30 days after treatment [16]. The GL2011 radioprotector has also been shown to induce enhanced expression of proteins and antioxidant enzymes, including vimentin, septin-5, voltage-dependent anion selective channel protein and superoxide dismutase 2 [15].

The main goal of the present study was to focus on brain tissue of irradiated animals and to examine molecular and cellular changes that occur with or without the application of the GL2011 radioprotector. Thus, an innovative approach using Raman microscopy was used to reveal its molecular signatures, while neuroglia, microglia and astrocytes, as cellular biomarkers of neuroinflammation, were followed

immunohistochemically. The brainstem was chosen since it is one of the most radiosensitive structures of the central nervous system [17] and because it is the central regulator of essential bodily states and functions, including respiratory and cardiovascular rhythms and blood pressure [18]. The existence of a bidirectional communication between the brain and the peripheral immune system is established [19], and follow-up of the levels of cytokines in the periphery may help in monitoring the recovery of injured CNS [20]. Therefore the overall effect of the radioprotector on neuroinflammation, as indicated by the levels of pro- and anti-inflammatory cytokines, was also followed.

MATERIALS AND METHODS

Animals

Experiments were performed on two-month-old male albino Wistar rats, weighing about 200 g. Male rats were chosen in order to avoid possible variability due to the estrous cycle of females and to keep the number of animals to a minimum (in compliance with the 3 Rs principle). The animals were kept under standard laboratory conditions (room temperature $21 \pm 1^\circ\text{C}$, humidity 30%, and a 12-h light/dark cycle) with food and tap water provided *ad libitum*. The protocols for animal housing and maintenance were in accordance with the European Directive 2010/63/EU [21] and the national regulations on the protection of animals used for scientific purposes. Experiments and ethical evaluation of the project were approved by the Ethics Committee of the Faculty of Biology, University of Belgrade (approval number EK-BF-2016/08).

Experimental design

Six experimental groups were formed. The control group (CTRL) received neither radiation nor the radioprotector. The irradiated group (Irr) consisted of irradiated animals only, while the radioprotector control group (GL) was treated with the radioprotector GL2011 (100 mg/kg i.p.) only and received no radiation. The dosage of the radioprotector was established in our previous study [15]. In order to assess the molecular and cellular markers of radioprotection by one administration of GL2011 at different times,

three additional experimental groups were formed as follows: (i) GL2011 was administered 30 min prior to irradiation exposure (GLIr-30); (ii) 180 min post-irradiation (GLIr180); (iii) 360 min post-irradiation (GLIr360). The experimental timeline for studying the radioprotective potential of GL2011 is shown in Supplementary Fig. S1.

Treatment with gamma radiation

A 60-cobalt (^{60}Co) gamma-ray source was used for irradiation. Non-anesthetized immobilized animals were positioned in individual cages made of wire and arranged in a circle around the source (6 rats per session). The distance from the source was 25 cm, as per [22], where a similar setup and source were used. Body irradiation was performed with rats placed sideways to the source. The animals received 6.7 Gy radiation at a dose rate (0.41 Gy/min), which, based on literature data, corresponds to a $\text{LD}_{50/30}$ dose [22-24]. In the middle of a course of radiation treatment, the cages with rats were sideways rotated by 180° to provide uniform, whole-body irradiation. The surviving animals were euthanized on day 30 and their tissue was used for further analysis. Animals that did not survive the 30 days were not included in further analyses.

Survival analysis

The survival of animals was monitored throughout the experiment (30 days) in animals prepared for immunohistochemistry and enzyme-linked immunosorbent assay (ELISA). Each of the experimental groups comprised 4 animals each (overall $n=20$), except the irradiated group where $n=8$, in order to retain enough animals for further analyses.

Raman spectroscopy

Rat brainstems on day 30 were dissected out and stored at -80°C in preparation for Raman microspectroscopy. Prior to the collection of Raman spectra, the brainstems were cut into 20 μm -thick coronal sections on a cryotome (Leica Microsystems, Germany). Sections were mounted on calcium fluoride (CaF_2) microscope slides. Micro-Raman spectra of all investigated samples were recorded using a DXR Raman

Microscope (Thermo Scientific, USA). Samples were excited with a 785 nm diode laser at a power density of 14 mW. Backscattered Raman emissions were collected through an Olympus microscope with infinity-corrected confocal optics, a 25- μm pinhole aperture, a standard working distance objective 50, a grid of 1800 lines/mm and a resolution of 2 cm^{-1} . The acquisition time was 60 s with 20 scans. Spectra were recorded within the same section of the rat gigantocellular reticular nucleus to minimize the impact of tissue inhomogeneity on the Raman readout. The spectral range was 600-1800 cm^{-1} . Thermo Scientific OMNIC software was used for spectra collection. Cutting out of spike artefacts from cosmic rays was performed in Spectragryph spectroscopy software ver. 1.2. Raman spectra were normalized to the maximum signal intensity using Matlab[®] 2010a package "Raman processing" [25]. The background signal was corrected using a median filter. The spectrum intensities were compared by plotting the mean spectra of groups and the mean differences of the spectra between groups. Further analysis of Raman spectra included the assignment of bands and the assessment of statistical significance of their differences. Six animals per experimental group (overall $n=36$ animals) were used for Raman spectral analysis and five spectra per tissue section were recorded.

Immunohistochemistry

The animals that survived up until the 30th day were anesthetized with a weight-dependent dose of 10% ketamine (Richter pharma AG, Wels, Austria) and 2% xylazine (Bioveta a.s., Ivanovice na Hane, Czech Republic) dissolved as 0.1 mL/100 g b.w. After losing the pedal withdrawal reflex (a marker for deep anesthesia), the rats were placed in the supine position and transcardially perfused with physiological solution (0.9% NaCl) and 4% paraformaldehyde in 0.1 M phosphate buffer, pH 7.4, followed by decapitation with a guillotine.

The brainstems were submerged in 4% paraformaldehyde for 24 h at 4°C , and then transferred to a 30% sucrose solution (in 0.1 M phosphate buffer) until further processing. Before cutting, the brains were kept at -80°C for 24 h. Tissue sections (30 μm) were cut by a cryostat (Leica, Microsystems,

Germany) mounted on microscope slides (Superfrost Plus, Thermo Scientific, USA) and stored at 4°C until staining. The sections were washed three times with 0.01 M phosphate buffer saline (PBS, pH 7.4). To prevent nonspecific binding, the sections were incubated in a blocking solution (10% bovine serum albumin (BSA) in PBS with 0.2% Triton X-100) for 1 h at room temperature (RT). After blocking, the sections were incubated overnight at 4°C with primary antibodies diluted in 2% BSA blocking solution (the marker of microglial cells or polyclonal goat anti-ionized calcium-binding adaptor molecule 1 (Iba-1) Abcam, USA 1:250; the marker of astrocytes or polyclonal rabbit anti-gial fibrillary acidic protein (GFAP) Dako, USA). On the second day, after 5 washes with PBS the sections were incubated with appropriate fluorophore-conjugated secondary antibodies for 2 h at RT (Alexa Fluor 488 donkey-anti goat; Alexa Fluor 555 donkey-anti rabbit; Invitrogen, USA). After the washing steps with PBS, the sections were stained with TO-PRO nuclear stain (1:4000, Thermo Fisher, USA). The negative control for Iba-1 and GFAP was obtained by eliminating the primary antibodies. Image acquisition was performed on a confocal laser scanning microscope LSM 510 (Zeiss, Germany) in multitrack configuration, with the objective lens Plan-Apochromat 40× for oil immersion. Confocal imaging was performed with an argon laser (488 nm), two helium-neon lasers (543 and 633 nm), and a dichroic mirror (488/543/633) with a bandpass filter at 505-530 and two long pass filters at 585 and 650 nm. Image J software was used for analysis of the obtained images. The images were converted to 8-bit; the channels were split and the auto-threshold was adjusted. The areas under antibody reactions were selected to quantify the number of pixels (in percentages) per image frame. This type of analysis was carried out on three animals per group (n=3), two sections per animal. Four images were taken per section.

Evaluation of plasma cytokine levels by ELISA

The levels of cytokines (TNF- α , IL-6, and IL-10) were measured in the plasma of control and treated animals by ELISA (R&D Systems, Minneapolis, USA) according to the manufacturer's instructions. Blood samples were taken from the tail vein on the 1st, 7th and 28th days. The blood of each animal was collected

in separate Eppendorf tubes precoated with EDTA (10 μ L 0.5 M EDTA per 1 mL of blood). Two mL of blood were taken from each animal, after which the contents were gently mixed and incubated for 30 min on ice. After 20 min of centrifugation at 4°C, 2000 \times g, the supernatant (blood plasma) was transferred to new Eppendorf tubes and deep-frozen at -80°C until the assay. Cytokine concentrations were calculated by a referent standard curve constructed using known amounts of set-provided recombinant cytokines. Out of the 3 planned blood collection time points (ELISA days 1, 7 and 28), we successfully completed the first two blood collection points (on days 1 and 7) with all experimental animal groups. However, on the final 28th day, there were n=3 for Irr, GLIr-30, GLIr180, and GLIr360, while n=4 remained for CTRL and GL.

Statistical analysis

Statistical analysis was performed using SPSS Statistics, 18.0 (SPSS Inc., Chicago, USA). The survival of animals was tested using Fisher's nonparametric test. The data from Raman microspectroscopy were analyzed using the Kruskal-Wallis ANOVA on ranks, followed by Dunn's post hoc test, while the data from immunohistochemistry and ELISA were analyzed using one-way ANOVA, followed by the LSD and Holm-Sidak post hoc test of comparison. The data are presented as the mean \pm standard error of the mean (SEM). The difference between groups was considered statistically significant for P<0.05.

RESULTS

Survival analysis

Although we previously demonstrated the effect of GL2011 on the survival of equally irradiated animals [15], we aimed here to confirm these data with a different dosage protocol, albeit on a smaller number of animals (pertaining to the 3Rs principle). Out of 28 experimental animals monitored for survival, 8 animals died before the final 30th day. In the control group of animals (CTRL), as well as in the non-irradiated group receiving GL2011 only (GL), the survival rate was 100% (n=4/4), while in the group of irradiated animals in which GL2011 was omitted (Irr),

the survival rate was 37.5% ($n=3/8$; $P<0.05$). In the remaining three experimental groups where the radioprotector GL2011 was regularly paired with gamma radiation (GLIr-30, GLIr180, and GLIr360), 1 out of 4 animals in all groups died, hence the survival percentage was the same, 75% ($n=3/4$). All animal deaths occurred between the 12th and 16th days post radiation. The survival curve for all experimental groups is presented in Supplementary Fig. S2.

Raman spectra analysis

We employed an innovative approach using Raman microspectroscopy to define the molecular changes in rat brainstem tissue without fixation and without any labeling. Thus, in one spectroscopic scan of a microscopically defined tissue area we obtained a composite molecular fingerprint for a particular sample.

The average Raman spectrum of control rat brainstem tissue (CTRL) is shown in Fig. 1. The assignment of the most pronounced spectral bands was performed as described [26]. Briefly, the dominant bands were either from lipid compounds (1064 , 1304 , 1437 cm^{-1}), or from the combined contributions of lipids and proteins (1128 , 1270 , 1344 and 1657 cm^{-1}). Smaller but defined bands were attributed to cholesterol (702 cm^{-1}), phenylalanine (1003 cm^{-1}), tryptophan (759 and 1619 cm^{-1}) and nucleic acids (959 , 1373 cm^{-1}).

The spectra of the irradiated tissue displayed a fine difference from those of control tissue. The difference spectra (Fig. 2A) revealed a slight increase in the intensity of the phenylalanine (1003 cm^{-1}) and a decrease in bands assigned to lipid and protein deformation (1344 cm^{-1} , 1657 cm^{-1}), tryptophan (759 cm^{-1}) and nucleic acids (959 cm^{-1}). The brainstem of rats treated only with GL2011 did not differ from the control group (not shown).

The difference spectra between control and irradiated tissue after 30 min of pre-administration with GL2011 (Fig. 2B) pinpoints the decrease in intensity of bands attributed to cholesterol, adenine, thymine

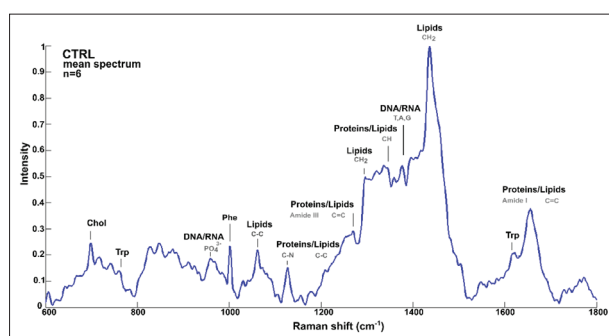


Fig. 1. Average Raman spectra of control rat brainstem tissue with the most pronounced bands: Chol – cholesterol (702 cm^{-1}), Trp – tryptophan (759 , 1619 cm^{-1}), DNA/RNA, symmetric stretching vibration of PO_4^{3-} (959 cm^{-1}), Phe – phenylalanine (1003 cm^{-1}), skeletal C-C stretch of lipids (1064 cm^{-1}), C-N stretching of proteins and C-C skeletal acyl backbone in lipids (1128 cm^{-1}), amide III band in proteins (C-N stretch from α -helix) and C=C groups in unsaturated fatty acids and phospholipids (1270 cm^{-1}), CH_2 deformation band in lipid (1304 cm^{-1}), C-H deformation band in proteins and lipids (1344 cm^{-1}), T, A, G – ring breathing modes of the DNA/RNA bases thymine, adenine, guanine (1373 cm^{-1}), CH_2 deformation band in lipids (1437 cm^{-1}), amide I band of proteins, C=C group in lipids (1657 cm^{-1}).

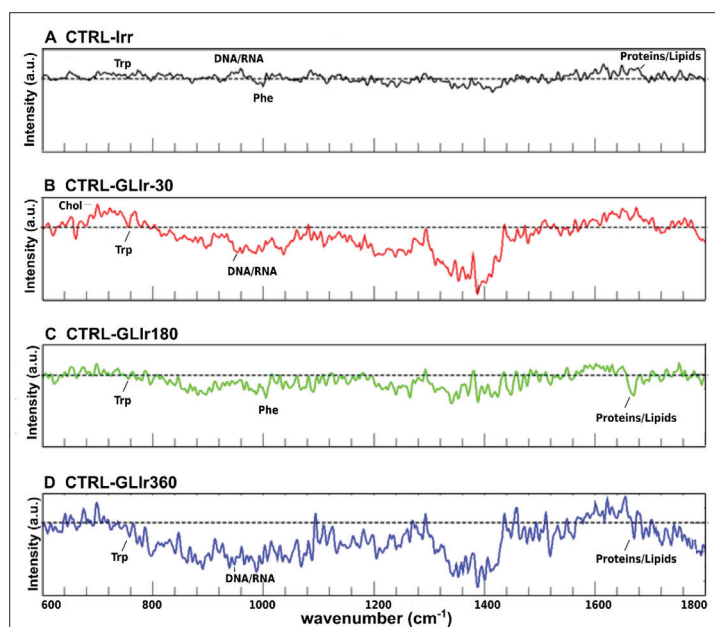


Fig. 2. Difference spectra between control and A – irradiated rat brainstem tissue (no protection); B – irradiated tissue with radioprotector administered 30 min before the irradiation (group GLIr-30); C – irradiated tissue with radioprotector administered 3 h after irradiation (group GLIr180); D – irradiated tissue with radioprotector administered 6 h after irradiation (group GLIr360). Trp – tryptophan (759 cm^{-1}), DNA/RNA (959 cm^{-1}), Phe – phenylalanine (1003 cm^{-1}), Chol – cholesterol (702 cm^{-1}). Dashed horizontal line denote zero difference. Negative values (below the dashed horizontal line) denote lower values than the control. Positive values (above the dashed horizontal line) denote higher values than the control.

and tryptophan, while the bands assigned to phenylalanine, lipids and nucleic acids showed a relative increase in intensity. Similar changes in the intensities of bands as in GLIr-30 were observed in GLIr180 and GLIr360 spectra (Fig. 2C, D, respectively). The intensity of the band assigned to phenylalanine (1003 cm^{-1}) showed a steady increase compared to CTRL in all GL2011 experimental groups. The band attributed to tryptophan (759 cm^{-1}) diminished in intensity in the GLIr-30 group when compared to the CTRL (Fig. 2B), while it increased in GLIr180 and GLIr360 groups (Fig. 2C, D, respectively). The same change in pattern was detected in the band at 1657 cm^{-1} and assigned to amide I (not shown), which could suggest an association with the level of tryptophan. The intensity of bands related to nucleic acids was slightly diminished in irradiated tissue, and it rose significantly after treatment with GL2011 either before or after irradiation.

The effect of radiation and radioprotector treatments on the normalized intensities of the bands assigned to tryptophan, nucleic acids and phenylalanine, ones that exhibited significant spectral differences as compared to the control and Irr groups, are shown in Fig. 3. There was a significant difference (compared to Irr) in the intensity of the tryptophan band at 759 cm^{-1} for the GL2011 treatment at 3h (GLIr180) and 6h (GLIr360) after irradiation (Fig. 3A). A gradual increase in this band accompanied the delay in radioprotector application. For the tryptophan band, the GLIr360 group also showed a difference compared to the CTRL (Fig. 3A). A significant difference was found in the intensity of the nucleic acid band (959 cm^{-1}) between the Irr group and each irradiated and radioprotector-treated group (Fig. 3B), as well as between CTRL and GLIr-30 and GLIr360. Here the radioprotector treatment seemed to induce the same effect regardless of the timing (Fig. 4B). With regard to the intensity of the phenylalanine band (1003 cm^{-1}), there was a significant difference (compared to Irr) for radioprotector treatment 30 min prior to irradiation (GLIr-30) and 6 h (GLIr360) post-irradiation (Fig. 3C). In addition, the increased intensity of the phenylalanine band in each irradiated and GL2011-treated group of animals (GLIr-30, GLIr180 and GLIr360) was significant in comparison with the CTRL group (Fig. 3C).

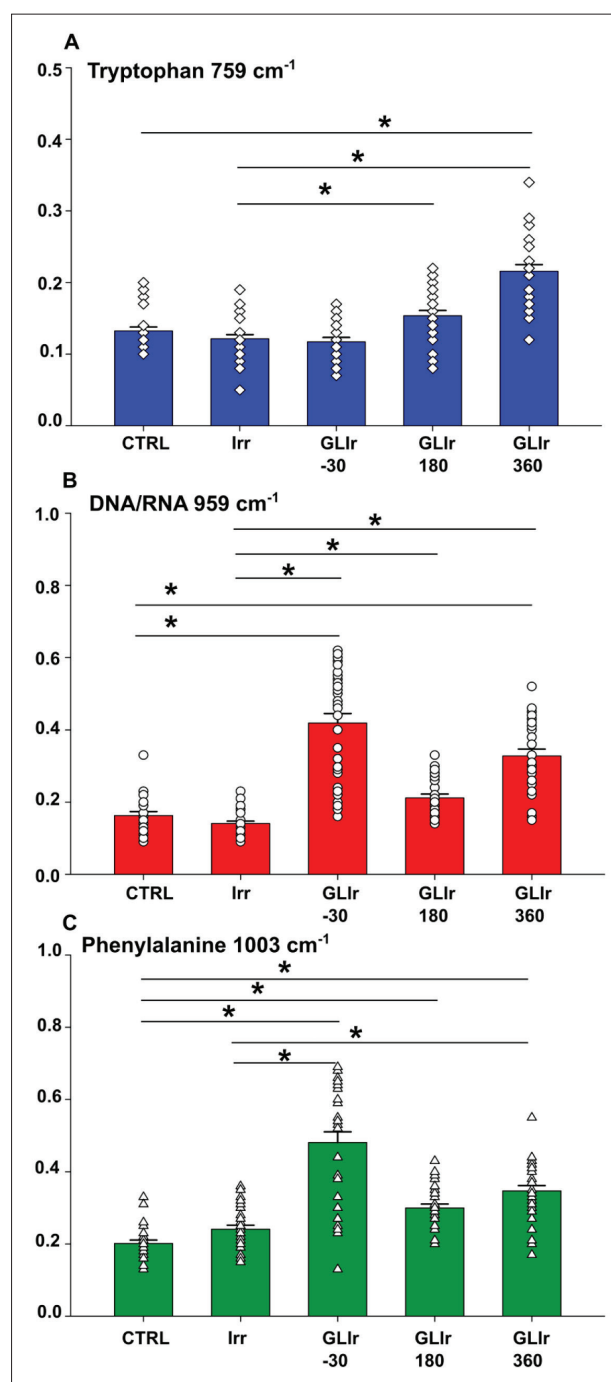


Fig. 3. Mean Raman band intensities with significances assigned to tryptophan (A), nucleic acids (B) and phenylalanine (C). Statistical analysis was performed using the Kruskal-Wallis ANOVA on ranks with Dunn's post hoc test. Data are presented as the mean \pm SEM, * $P < 0.05$.

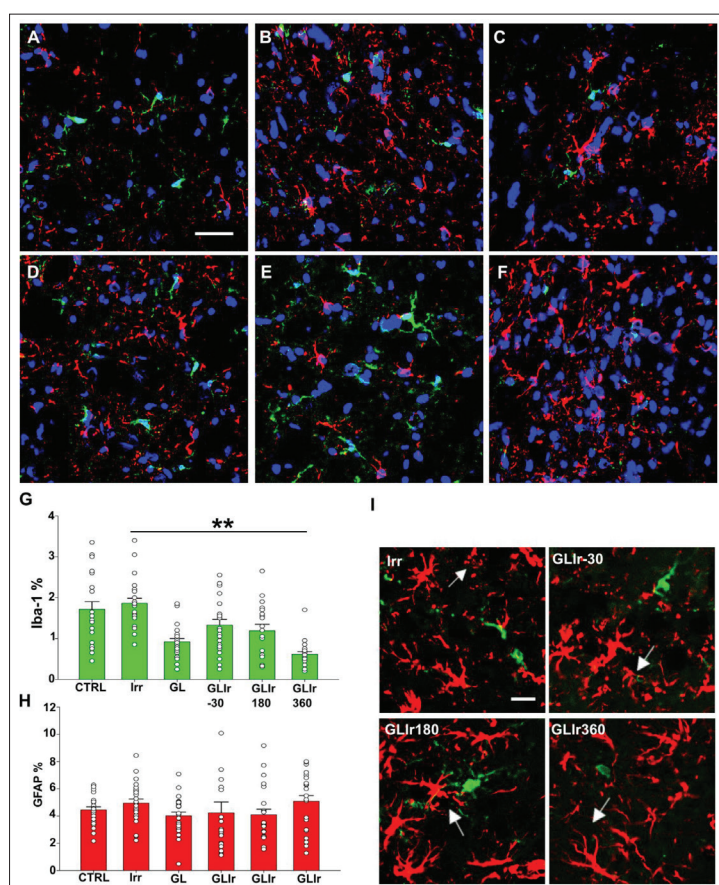


Fig. 4. Immunohistochemical staining of the rat brainstem; gigantocellular reticular nucleus. Iba-1, microglia marker (green), GFAP, astrocyte marker (red) and TO-PRO nuclear stain (blue). **A** – Control group (CTRL). **B** – Irradiated animals without any protection (Irr). **C** – Radioprotector only group (GL). **D** – Animals treated with the radioprotector GL2011 30 minutes before irradiation (GLIr-30). **E** – Animals treated with GL2011 180 min after irradiation (GLIr180). **F** – Animals treated with GL2011 360 min after irradiation (GLIr360). Scale bar in images A-F – 40 μ m. **G, H** – Quantitative comparison of immunohistochemical staining of brainstem tissue presented as the mean \pm SEM among the six groups CTRL, Irr, GL, GLIr-30, GLIr180 and GLIr360. The number of pixels of the Iba-1 (**G**) and GFAP (**H**) staining areas expressed as percentages of the image frame area. **I** – Representative confocal images of Irr, GLIr-30, GLIr180 and GLIr360, scale bar 20 μ m (arrows indicate dystrophic astrocytes in Irr, GLIr-30 and recovered astrocytes in GLIr180 and GLIr360). Statistical analysis was performed using one-way ANOVA, followed by the LSD post hoc test. Data are presented as the mean \pm SEM, ** $P < 0.01$.

The response of neuroglia

In animals that were irradiated (Fig. 4B), indications of Iba-1 positive microglia with scarcely observable cellular processes were observed, as well as a slight but not significant increase of the percentage of Iba-1 occupied area when compared to CTRL (Fig. 4A).

Depending on the timing of GL2011 application, microglial cells exhibited different changes in morphology. The animals treated with the radioprotector 30 min before irradiation showed indications of an inflammatory phenotype, which was reflected by the continued retraction of microglial processes (Fig. 4D). In preparations from animals treated with the radioprotector 3 h after irradiation (GLIr180), some increase in some of microglial cells could be observed (Fig. 4E), while in the GLIr360 group, microglial cells displayed a relatively smaller somatic size (Fig. 4F). Only the latter GLIr360 treatment group showed a significant ($P < 0.01$) change in the Iba-1-stained area (Fig. 4G) when compared to the Irr group. The radioprotector alone did not produce any outstanding changes in microglial morphology (Fig. 4C), however, a decrease in Iba-1 staining was observed, but it was not significant (Fig. 4G).

Although assessment of the astrocyte marker GFAP (Fig. 4H) did not demonstrate any significant differences between groups, changes in the astrocyte phenotype due to irradiation were noted. More precisely, we observed an apparent fragmentation of astrocyte processes in the tissue samples of irradiated animals (Fig. 4B). A similar appearance of dystrophic-like astrocytes were detected in tissue samples of animals treated with the radioprotector 30 min prior to irradiation (Fig. 4D, I). When compared with the morphology of astrocytes in the Irr and GLIr-30 groups, application of the radioprotector 3 h and 6 h after irradiation led to a more compact shape of astrocytes (Fig. 4E, F, I). We did not observe a change in the astrocyte phenotype in the group of animals receiving only the radioprotector treatment (GL group, Fig. 4C).

Effect of radiation and GL2011 on plasma cytokine levels

Irradiation induced increases in plasma IL-6 levels on the 1st and 7th days post-irradiation, with the difference

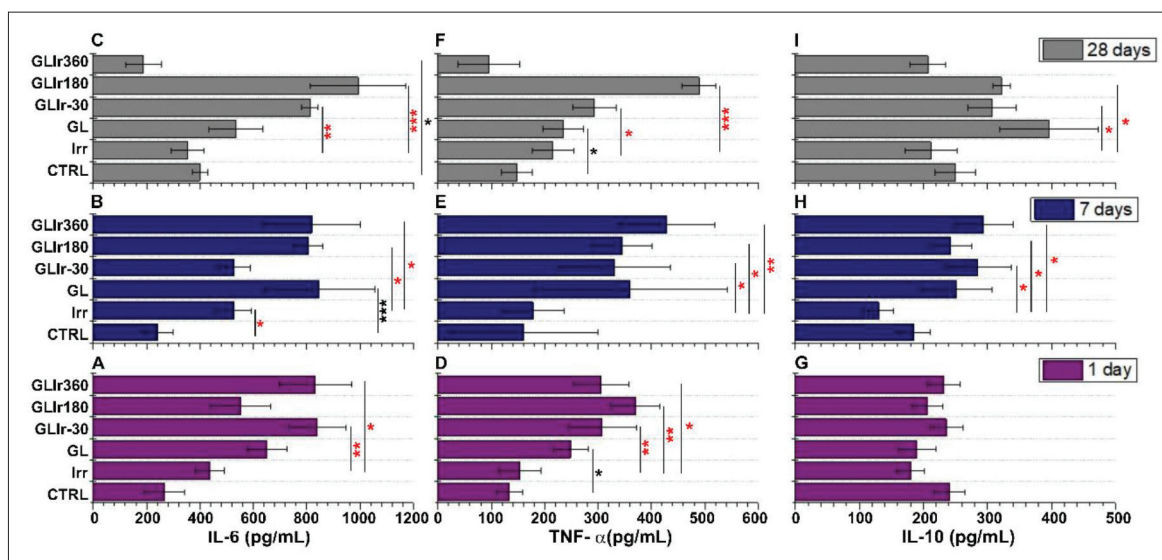


Fig. 5. Effect of irradiation and treatment with radioprotector GL2011 on plasma cytokine levels. Data presented as mean±SEM from rats/CTRL or the treated group. **A** – IL-6 on the 1st day; **B** – IL-6 on the 7th day; **C** – IL-6 on the 28th day; **D** – TNF- α on the 1st day; **E** – TNF- α on the 7th day; **F** – TNF- α on the 28th day; **G** – IL-10 on the 1st day; **H** – IL-10 on the 7th day; **I** – IL-10 on the 28th day. Statistical analysis was performed using one-way ANOVA, followed by the Holm-Sidak post hoc test. * $P < 0.05$, ** $P < 0.01$, *** $P < 0.001$ (red asterisks: difference compared to Irr).

being statistically significant on the 7th day only (Fig. 5B). A further significant increase was seen in plasma IL-6 levels in the GLIr-30 group as compared to the Irr group on the 1st and 28th days after treatment (Fig. 5A, C, respectively). A higher plasma IL-6 level was also observed for GLIr180, but it was only significant at later time points, on the 7th and 28th days (Fig. 5B, C, respectively). Similarly, the GLIr360 group showed a significant increase in IL-6 in comparison to the Irr group on the 1st and 7th days after treatment (Fig. 5A, B, respectively). Surprisingly, on the 28th day, the last point in time, analysis of plasma IL-6 levels in the GLIr360 group revealed a significantly lower value as compared to the CTRL (Fig. 5C). GL2011 alone (GL group) also caused an increase in the plasma level of IL-6 but achieved significance in comparison to the CTRL only on the 7th day after treatment (Fig. 5B).

Irradiation did not induce a significant increase in TNF- α level. However, when compared to the Irr group, a significant increase in TNF- α level was detected in all irradiated groups with the radioprotector on the 1st and 7th days after treatment (Fig. 5D, E, respectively). At later time points, this increase was significant for the GLIr-30 and GLIr180 groups on the 28th day (Fig. 5F). The radioprotector alone (the GL group) caused an increase in TNF- α level at all time

points, with a significant difference with respect to the CTRL observed on the 1st and 28th days (Fig. 5D, F, respectively).

The plasma levels of anti-inflammatory IL-10 were similar in all experimental groups, with no significant differences observed between groups on the 1st day (Fig. 5G). However, on the 7th day (Fig. 5H), a significantly higher level of IL-10 was detected in all protected groups as compared to the Irr group, while on the 28th day, IL-10 remained significantly higher in the GLIr-30 and GLIr180 groups (Fig. 5I).

DISCUSSION

Radiation exposure can directly or indirectly affect the brain by damaging tissue through several mechanisms: the production of reactive oxygen species (ROS), oxidative damage and lesions in the DNA molecule, as well as through mutations that can lead to carcinogenesis or cell death [27]. In this study, we followed the protective effect of a new natural aminothiol radioprotector, GL2011, by following the changes that occur in the brainstem at the cellular and molecular levels after irradiation/radioprotection. In a previous study [15], we showed that the administration of

GL2011 at three identical doses at three time points resulted in the improvement of the survival rate of irradiated rats. In the present study, we confirmed the improvement of rat survival, even after application of one dose at different times. These findings primarily indicate that GL2011 could elicit radioprotective changes in the brain when applied after a radiation incident as well as before radiation exposure.

It was shown that murine brains exposed to 10 Gy of gamma radiation expressed strong Raman spectral changes [28]. In another study performed on male Wistar rats, three-model whole-body dosages of gamma rays were used: 14.4 Gy, 9.6 Gy, and 4.8 Gy [29]; the lower lethal dose (9.6 Gy) was used to prolong the time of observation, delaying the time of death to the 10th day, while the dose of 4.8 Gy did not cause significant changes in the examined marker, melatonin of the pineal gland. In the present study, we used 6.7 Gy as a mild dose for which Raman microspectroscopy did not reveal significant differences from the control spectra. However, Raman spectra revealed some interesting molecular signatures for the effects of different radioprotector treatments as compared to the control.

In contrast to application prior to radiation (GLIr-30), an increase in the protein band with a strong lipid contribution (1657 cm^{-1}) occurred when the application of the radioprotector was delayed, i.e. administered post-irradiation (3 h or 6 h), highlighting the protective action of GL2011. The increase in intensity of this protein band could be explained in part by the irradiation-induced activation of transcription factors, which in turn control the gene expression of proinflammatory cytokines such as TNF- α , IL-1, IL-6, and anti-inflammatory cytokines such as IL-4, IL-10, IL-13 and TGF- β [30,31]. This is congruent with our finding of an increase in the levels of IL-6, TNF- α and IL-10 after application of GL2011.

The increase in intensity of the band at 959 cm^{-1} that was observed at all three time points of radioprotector application revealed an increase in the level of nucleic acids. Considering that increased levels of proteins were determined in the radioprotected groups GLIr180 and GLIr360, this could be related to a rise in iRNA as evidenced in the Raman band for nucleic acids. These findings on radiation-associated molecular damage in rat brainstem parenchyma are in

agreement with the previously reported radioprotective enhancement of nucleic acid repair and inhibition of cell death [32].

The increase in phenylalanine in all groups of treated animals could be explained by a change in the metabolism of this amino acid. Some proinflammatory cytokines, particularly IL-6 (which is significantly increased in the blood plasma of GL2011-treated rats), block the conversion of phenylalanine to tyrosine [33], hence the increase in the level of the former amino acid.

The level of tryptophan according to Raman spectra followed the trend of nucleic acids and proteins. Although there was no significant change in its band after radiation, it is known that proinflammatory cytokines, such as IL-6 (which was increased in the Irr group on the 7th day) could lead to degradation of tryptophan [34,35]. It is of interest to note a compensatory rise in the level of tryptophan in GLIr180 and GLIr360 groups as compared to irradiated animals.

To follow the cellular response to radiation and radioprotection and the underlining neuroinflammation, tissue sections were immunostained for microglia and astrocytes. Microglial cells are the main cellular component involved in the innate immune defense of the central nervous system [36]. Reactivation of microglial cells is characterized by their acquisition of an amoeboid shape in many pathological states, and the reduction in the number of processes is one of the defining characteristics of activated microglia [37]. However, the irradiation protocol used in our study showed that 30 days after irradiation, microglial cells in the brainstem underwent only a modest change in morphology, characterized by scarce cell processes, with no significant change in the percentage of the area occupied by the Iba-1 signal. Nevertheless, the radioprotector itself caused some suppression of the microglial marker (that can also be shared with macrophages), an effect that also occurred significantly if GL2011 was applied 6 h after irradiation, indicating a general inhibitory effect of the radioprotector on microglial proliferation. However, the administration of only GL2011 (GL group) had no apparent effect on microglial morphology, underlining the minimal invasiveness of the radioprotector towards glial cells.

Astrocytes are widely distributed in the brain, with numerous functions including structural support

in the CNS, maintenance of hemodynamics as well as secretion of a variety of cytokines [38,39]. Astrocytes also support neuronal survival by protecting them from oxidative injury. This protective role arises from their relatively high content of antioxidants [40], and to inhibit inflammatory processes in the brain, they also produce soluble factors that inhibit microglial activation, such as the TGF- β and prostaglandins [41,42]. Studies have reported that doses above LD₅₀, typically greater than 10 Gy, increase the presence of GFAP-positive astrocytes, while lower doses, typically below 8 Gy, did not induce noticeable changes in GFAP, even 30 days after irradiation [43,44], which is in agreement with our quantitative data. Regarding the morphology of astrocytes, irradiation induced fragmentation and a dystrophic-like phenotype that remained after application of the radioprotector 30 min before irradiation, and was reminiscent of astrocyte damage but also of astrogliosis, which is considered to be a common response to general CNS damage [45]. Conversely, we observed that application of the radioprotector 3 h or 6 h after irradiation promoted a recovery of the astrocytic phenotype, suggesting that the application of GL2011 was more beneficial for astroglia if applied post-irradiation.

The brain and the immune system are in bidirectional communication, which is essential for maintaining homeostasis [46]. The brain modulates immune functions through autonomic and neuroendocrine pathways [47]. Neurotransmitters and hormones released by these neural pathways interact with immune cells to alter global immune functions, including cytokine production [48]. Radiation is known to activate cytokine complexes that function in a highly orchestrated way, enabling interactions between mesenchymal, epithelial and immune cells [49]. Proinflammatory cytokines are rapidly activated after tissue irradiation, subsequently generating free radicals, including ROS and reactive nitrogen species. This proinflammatory phase is sustained long after radiation exposure. The balance between pro- and anti-inflammatory responses can oscillate back and forth for a long time after irradiation, and is considered critical in determining a positive or a negative outcome [50].

Elevated levels of TNF- α have been found after irradiation of different human or mammalian cells,

such as alveolar macrophages or tumor cells, while the overproduction of IL-6 and IL-8 has been described in keratinocytes, fibroblasts and glioma cells after both X-ray or UV exposure [51]. Our results show a sustained increase in plasma proinflammatory cytokines, IL-6 in almost all the groups that were irradiated and received GL2011 under different application regimes, likewise TNF- α , but with a more persistent effect throughout the protected groups. Notably, the non-irradiated GL group (radioprotector only) generally also showed an increase in IL-6 and TNF- α at all times. AS101 (ammonium trichloro(dioxoethylene-O-O')tellurate), a member of another class of radioprotectors and immunomodulators, was found to stimulate the production of IL-1, IL-6 and TNF- α , which underlines its role [52]. Thus, in addition to the previously published aminothiols mechanisms of radioprotection [11,15,16], here we showed with GL2011 another function, related to the manipulation of cytokine pathways.

In our experiments, the Irr group exhibited a rise in IL-6 on the 1st day and a significantly higher level on the 7th day, which is similar to the findings that elevated IL-6 production increases with the dose of radiation, reaching a maximum effect later after irradiation [53]. On the other hand, IL-6 induces radiation resistance [54], and by acting as a multifunctional cytokine, it regulates the immune response, the acute phase response and inflammatory reactions and hematopoiesis [55]. In addition, it was observed that some cytokines (TNF- α and IL-6, among others) were highly represented in the conditioned medium of an irradiated glioblastoma cell line [56]. The significant rise in IL-6 and TNF- α levels concomitantly with IL-10 was noted in the GLIr180 group as compared to the Irr group, as well as in the GLIr-30 group. However, when measured on the final 28th day, the treatment with GL2011 6 h after radiation ceased to show an effect (as compared to Irr) for all inflammatory markers. On the 1st day after treatment, only the proinflammatory cytokines were activated, and on the 7th day this was counterbalanced by a rise in anti-inflammatory IL-10, which may indicate a healing effect with GL2011 at all treatment times. It is also worth noting that IL-6 can act in concert with IL-10 at the translational level, inhibiting TNF- α protein expression by astrocytes [57], which suggests that these humoral factors act as important regulators of other cytokines

whose actions could be detrimental to the brain. However, the rise in the level of a specific cytokine in a disease setting or following radiation does not necessarily indicate how cohorts of cytokines interact with one another or whether a specific cytokine is causally involved in inflammatory tissue damage [49].

The results of our study confirmed the increased survival of animals treated with GL2011 either before or after irradiation. On the molecular level, Raman microspectroscopy revealed that the radioprotector mostly stimulated the turnover of nucleic acids, while immunohistochemistry showed diminished infiltration of microglial cells, especially if GL2011 was applied after irradiation. A possible radioprotective effect was also indicated by the change in the pattern of cytokines release. These data suggest that the radioprotector GL2011, operating as an immune system modulator, protects the brainstem from the effect of whole-body radiation.

Funding: This work was supported by the Ministry of Education, Science and Technological Development, Republic of Serbia, Contract No. 451-03-68/2020-14/200178.

Acknowledgements: We are grateful to Prof. Dr. Gert Lubec, University of Vienna, Austria, who donated the GL2011 radioprotector, and to Miloš Jovanović for his help in animal care and handling. The authors are also grateful to the Institute of Anatomy, Faculty of Medicine, University of Belgrade, for access to the tissue processing equipment.

Author contributions: Conceptualization and supervision: MD, PRA and BBN; investigation and analysis: DMK, IM and DBB; writing-original draft: MD and DMK; writing-review and editing: PRA and BBN.

Conflict of interest disclosure: The authors declare that they have no competing interests.

REFERENCES

- Reisz JA, Bansal N, Qian J, Zhao W, Furdui CM. Effects of Ionizing Radiation on Biological Molecules - Mechanisms of Damage and Emerging Methods of Detection. *Antioxid Redox Signal*. 2014;21(2):260-92. <https://doi.org/10.1089/ars.2013.5489>
- Balentova S, Adamkov M. Molecular, Cellular and Functional Effects of Radiation-Induced Brain Injury: A Review. *Int J Mol Sci*. 2015;16(11):27796-815. <https://doi.org/10.3390/ijms161126068>
- Smart D. Radiation Toxicity in the Central Nervous System: Mechanisms and Strategies for Injury Reduction. *Semin Radiat Oncol*. 2017;27(4):332-9.
- White RJ, Abel S, Horne ZD, Lee J, Edington H, Greenberg L, Younes H, Hilton C, Wegner RE. Melanoma brain metastases: is it time to eliminate radiotherapy? *J Neurooncol*. 2020;149(1):27-33. <https://doi.org/10.1007/s11060-020-03485-w>
- Facorro G, Sarrasague MM, Torti H, Hager A, Avalos JS, Foncuberta M, Kusminsky G. Oxidative study of patients with total body irradiation: effects of amifostine treatment. *Bone Marrow Transplant*. 2004;33(8):793-8. <https://doi.org/10.1038/sj.bmt.1704427>
- Singh VK, Seed TM. The efficacy and safety of amifostine for the acute radiation syndrome. *Expert Opin Drug Saf*. 2019;18(11):1077-90. <https://doi.org/10.1080/14740338.2019.1666104>
- Vardy J, Wong E, Izard M, Clifford A, Clarke SJ. Life-threatening anaphylactoid reaction to amifostine used with concurrent chemoradiotherapy for nasopharyngeal cancer in a patient with dermatomyositis: a case report with literature review. *Anticancer Drugs*. 2002;13(3):327-30. <https://doi.org/10.1097/00001813-200203000-00015>
- Dziegielewski J, Goetz W, Baulch JE. Heavy ions, radioprotectors and genomic instability: implications for human space exploration. *Radiat Environ Biophys*. 2010;49(3):303-16. <https://doi.org/10.1007/s00411-009-0261-9>
- Singh VK, Romaine PLP, Seed TM. Medical Countermeasures for Radiation Exposure and Related Injuries: Characterization of Medicines, FDA-Approval Status and Inclusion into the Strategic National Stockpile. *Health Phys*. 2015;108(6):607-30. <https://doi.org/10.1097/hp.0000000000000279>
- Copp RR, Peebles DD, Soref CM, Fahl WE. Radioprotective efficacy and toxicity of a new family of aminothiols. *Int J Radiat Biol*. 2013;89(7):485-92. <https://doi.org/10.3109/09553002.2013.770579>
- Kuntić VS, Stanković MB, Vujić ZB, Brborić JS, Uskoković-Marković SM. Radioprotectors - the Evergreen Topic. *Chem Biodivers*. 2013;10(10):1791-803. <https://doi.org/10.1002/cbdv.201300054>
- Rosen EM, Day R, Singh VK. New Approaches to Radiation Protection. *Front Oncol*. 2015;4:381.
- Varanda EA, Tavares DC. Radioprotection: mechanisms and radioprotective agents including honeybee venom. *J Venom Anim Toxins*. 1998;4(1):5-21. <https://doi.org/10.1590/s0104-79301998000100002>
- Peebles DD, Soref CM, Copp RR, Thunberg AL, Fahl WE. ROS-Scavenger and Radioprotective Efficacy of the New PrC-210. *Aminothiol. Radiat Res*. 2012;178(1):57-68. <https://doi.org/10.1667/rr2806.1>
- Ganesan MK, Jovanovic M, Secerov B, Ignjatovic M, Bilban M, Pavle A, Refaei AE, Jung G, Li L, Sase A, Chen W, Bacic G, Lubec G. Radiation protection from whole-body gamma irradiation (6.7 Gy): behavioural effects and brain protein-level changes by an aminothiol compound GL2011 in the Wistar rat. *Amino Acids*. 2014;46(7):1681-96. <https://doi.org/10.1007/s00726-014-1728-9>
- Okić-Djordjević I, Trivanović D, Jovanović M, Ignjatović M, Šećerov B, Mojović M, Bugarski D, Bačić G, Andjus PR. Increased survival after irradiation followed by regeneration of bone marrow stromal cells with a novel

- thiol-based radioprotector. *Croat Med J.* 2014;55(1):45-9. <https://doi.org/10.3325/cmj.2014.55.45>
17. Scoccianti S, Detti B, Gadda D, Greto D, Furfaro I, Meacci F, Simontacchi G, Di Brina L, Bonomo P, Giacomelli I, Meattini I, Mangoni M, Cappelli S, Cassani S, Talamonti C, Bordi L, Livi L. Organs at risk in the brain and their dose-constraints in adults and in children: A radiation oncologist's guide for delineation in everyday practice. *Radiother Oncol.* 2015;114(2):230-8. <https://doi.org/10.1016/j.radonc.2015.01.016>
 18. Nicholls JG, Paton JFR. Brainstem: neural networks vital for life. *Philos Trans R Soc B Biol Sci.* 2009;364(1529):2447-51. <https://doi.org/10.1098/rstb.2009.0064>
 19. Träger U, Tabrizi SJ. Peripheral inflammation in neurodegeneration. *J Mol Med.* 2013;91(6):673-81.
 20. Rusiecki J, Levin LI, Wang L, Byrne C, Krishnamurthy J, Chen L, Galdzicki Z, French LM. Blast traumatic brain injury and serum inflammatory cytokines: a repeated measures case-control study among U.S. military service members. *J Neuroinflammation.* 2020;17(1):20. <https://doi.org/10.1186/s12974-019-1624-z>
 21. Directive 2010/63/EU of the European Parliament and of the Council of 22 September 2010 on the protection of animals used for scientific purposes Text with EEA relevance. *Off J Eur Un.* 2010;L276:33.
 22. Logie LC, Harris MD, Tatsch RE, van Hooser EN. An Analysis of the LD 50(30) as Related to Radiation Intensity. *Radiat Res.* 1960;12(4):349. <https://doi.org/10.2307/3571043>
 23. Basile LA, Ellefson D, Gluzman-Poltorak Z, Junes-Gill K, Mar V, Mendonca S, Miller JD, Tom J, Trinh A, Gallaher TK. HemaMax™, a Recombinant Human Interleukin-12, Is a Potent Mitigator of Acute Radiation Injury in Mice and Non-Human Primates. *PLoS ONE.* 2012;7(2):e30434. <https://doi.org/10.1371/journal.pone.0030434>
 24. Doan PL, Himburg HA, Helms K, Russell JL, Fixsen E, Quarmyne M, Harris JR, Deoliviera D, Sullivan JM, Chao NJ, Kirsch DG, Chute JP. Epidermal growth factor regulates hematopoietic regeneration after radiation injury. *Nat Med.* 2013;19(3):295-304. <https://doi.org/10.1038/nm.3070>
 25. Reisner LA, Cao A, Pandya AK. An integrated software system for processing, analyzing, and classifying Raman spectra. *Chemom Intell Lab Syst.* 2011;105(1):83-90. <https://doi.org/10.1016/j.chemolab.2010.09.011>
 26. Movasaghi Z, Rehman S, ur Rehman DrI. Fourier Transform Infrared (FTIR) Spectroscopy of Biological Tissues. *Appl Spectrosc Rev.* 2008;43(2):134-79. <https://doi.org/10.1080/05704920701829043>
 27. Hall EJ, Giaccia AJ. *Radiobiology for the radiologist.* 7th ed. Philadelphia: Wolters Kluwer Health/Lippincott Williams & Wilkins; 2012.
 28. Lakshmi RJ, Kartha VB, Krishna CM, Solomon JGR, Ullas G, Devi PU. Tissue Raman Spectroscopy for the Study of Radiation Damage: Brain Irradiation of Mice. *Radiat Res.* 2002;157(2):175-82. [https://doi.org/10.1667/0033-7587\(2002\)157\[0175:trsfts\]2.0.co;2](https://doi.org/10.1667/0033-7587(2002)157[0175:trsfts]2.0.co;2)
 29. Kassayová M, Ahlersová E, Ahlers I. Two-Phase Response of Rat Pineal Melatonin to Lethal Whole-Body Irradiation With Gamma Rays. *Physiol. Res.* 1999;48(3):227-230.
 30. Di Maggio F, Minafra L, Forte G, Cammarata F, Lio D, Messa C, Gilardi M, Bravatà V. Portrait of inflammatory response to ionizing radiation treatment. *J Inflamm.* 2015;12(1):14. <https://doi.org/10.1186/s12950-015-0058-3>
 31. Lumniczky K, Szatmári T, Sáfrány G. Ionizing Radiation-Induced Immune and Inflammatory Reactions in the Brain. *Front Immunol.* 2017;8:517. <https://doi.org/10.3389/fimmu.2017.00517>
 32. Mohd Saaya F, Katsube T, Xie Y, Tanaka K, Fujita K, Wang B. Research and Development of Radioprotective Agents: A Mini-Review. *Int J Radiol.* 2017;4(2):128-38. <https://doi.org/10.17554/j.issn.2313-3406.2017.04.41>
 33. Felger JC, Miller AH. Cytokine effects on the basal ganglia and dopamine function: The subcortical source of inflammatory malaise. *Front Neuroendocrinol.* 2012;33(3):315-27. <https://doi.org/10.1016/j.yfrne.2012.09.003>
 34. Grohmann U, Fallarino F, Bianchi R, Belladonna ML, Vacca C, Orabona C, Uyttenhove C, Fioretti MC, Puccetti P. IL-6 Inhibits the Tolerogenic Function of CD8 α + Dendritic Cells Expressing Indoleamine 2,3-Dioxygenase. *J Immunol.* 2001;167(2):708-14. <https://doi.org/10.4049/jimmunol.167.2.708>
 35. Hol JW, Stolker RJ, Klimek M, Stronks DL, Fekkes D. The tryptophan kynurenine pathway, neopterin and IL-6 during vulvectomy and abdominal hysterectomy. *J Biomed Sci.* 2014;21(1):102. <https://doi.org/10.1186/s12929-014-0102-2>
 36. Bachiller S, Jiménez-Ferrer I, Paulus A, Yang Y, Swanberg M, Deierborg T, Boza-Serrano A. Microglia in Neurological Diseases: A Road Map to Brain-Disease Dependent-Inflammatory Response. *Front Cell Neurosci.* 2018;12:488. <https://doi.org/10.3389/fncel.2018.00488>
 37. Lull ME, Block ML. Microglial activation and chronic neurodegeneration. *Neurotherapeutics.* 2010;7(4):354-65. <https://doi.org/10.1016/j.nurt.2010.05.014>
 38. Sofroniew MV, Vinters HV. Astrocytes: biology and pathology. *Acta Neuropathol (Berl).* 2010;119(1):7-35. <https://doi.org/10.1007/s00401-009-0619-8>
 39. Colombo E, Farina C. Astrocytes: Key Regulators of Neuroinflammation. *Trends Immunol.* 2016;37(9):608-20. <https://doi.org/10.1016/j.it.2016.06.006>
 40. Wilson JX. Antioxidant defense of the brain: a role for astrocytes. *Can J Physiol Pharmacol.* 1997;75(10-11):1149-63. <https://doi.org/10.1139/y97-146>
 41. Vincent VAM, Tilders FJH. Inhibition of Endotoxin-Induced Nitric Oxide Synthase Production in Microglial Cells by the Presence of Astroglial Cells: A Role for Transforming Growth Factor β . *GLIA.* 1997;19(3):190-8. [https://doi.org/10.1002/\(sici\)1098-1136\(199703\)19:3<190::aid-glia2>3.0.co;2-3](https://doi.org/10.1002/(sici)1098-1136(199703)19:3<190::aid-glia2>3.0.co;2-3)
 42. Park SJ, Lee JH, Kim HY, Choi YH, Park JS, Suh YH, Park SM, Joe E, Jou I. Astrocytes, but Not Microglia, Rapidly Sense H₂O₂ via STAT6 Phosphorylation, Resulting in Cyclooxygenase-2 Expression and Prostaglandin Release. *J Immunol.* 2012;188(10):5132-41. <https://doi.org/10.4049/jimmunol.1101600>
 43. Mildenerberger M, Beach TG, McGeer EG, Ludgate CM. An animal model of prophylactic cranial irradiation: Histologic effects at acute, early and delayed stages. *Int J Radiat Oncol.* 1990;18(5):1051-60. [https://doi.org/10.1016/0360-3016\(90\)90440-u](https://doi.org/10.1016/0360-3016(90)90440-u)

44. Chiang CS, McBride WH, Withers HR. Radiation-induced astrocytic and microglial responses in mouse brain. *Radiother Oncol.* 1993;29(1):60-8. [https://doi.org/10.1016/0167-8140\(93\)90174-7](https://doi.org/10.1016/0167-8140(93)90174-7)
45. Li K, Li J, Zheng J, Qin S. Reactive Astrocytes in Neurodegenerative Diseases. *Aging Dis.* 2019;10(3):664-675. <https://doi.org/10.14336/ad.2018.0720>
46. Dantzer R. Neuroimmune Interactions: From the Brain to the Immune System and Vice Versa. *Physiol Rev.* 2018;98(1):477-504. <https://doi.org/10.1152/physrev.00039.2016>
47. Kenney MJ, Ganta CK. Autonomic Nervous System and Immune System Interactions. *Comprehensive Physiology.* 2014;4(3): 1177-200. <https://doi.org/10.1002/cphy.c130051>
48. Thyaga SR, Priyanka HP. Bidirectional communication between the neuroendocrine system and the immune system: relevance to health and diseases. *Ann Neurosci.* 2012;19(1):40-46. <https://doi.org/10.5214/ans.0972.7531.180410>
49. Schae D, Kachikwu EL, McBride WH. Cytokines in Radiobiological Responses: A Review. *Radiat Res.* 2012;178(6):505-23. <https://doi.org/10.1667/rr3031.1>
50. Sun Y, Cheng M-K, Griffiths TRL, Mellon JK, Kriajevska M, Manson MM. Inhibition of STAT Signalling in Bladder Cancer by Diindolylmethane - Relevance to Cell Adhesion, Migration and Proliferation. *Curr Cancer Drug Targets.* 2013;13(1):57-68. <https://doi.org/10.2174/156800913804486610>
51. Müller K, Meineke V. Radiation-induced alterations in cytokine production by skin cells. *Exp Hematol.* 2007;35(4):96-104. <https://doi.org/10.1016/j.exphem.2007.01.017>
52. Kalechman Y, Albeck M, Oron M, Sobelman D, Gurwith M, Seghal SN, Sredni B. Radioprotective effects of the immunomodulator AS101. *J Immunol.* 1990;145(5):1512-7.
53. Meeren AVD, Bertho J-M, Vandamme M, Gaugler M-H. Ionizing radiation enhances IL-6 and IL-8 production by human endothelial cells. *Mediators Inflamm.* 1997;6(3):185-93. <https://doi.org/10.1080/09629359791677>
54. Wu C-T, Chen M-F, Chen W-C, Hsieh C-C. The role of IL-6 in the radiation response of prostate cancer. *Radiat Oncol.* 2013;8(1):159.
55. Hirano T. Interleukin 6 and its Receptor: Ten Years Later. *Int Rev Immunol.* 1998;16(3-4):249-84.
56. Desai S, Kumar A, Laskar S, Pandey BN. Cytokine profile of conditioned medium from human tumor cell lines after acute and fractionated doses of gamma radiation and its effect on survival of bystander tumor cells. *Cytokine.* 2013;61(1):54-62. <https://doi.org/10.1016/j.cyto.2012.08.022>
57. Benveniste E-IN, Tang LP, Law RM. Differential regulation of astrocyte TNF- α expression by the cytokines TGF- β , IL-6 and IL-10. *Int J Devl Neurosci.* 1995;13(3-4):341-9. [https://doi.org/10.1016/0736-5748\(94\)00061-7](https://doi.org/10.1016/0736-5748(94)00061-7)

Supplementary Material

The Supplementary Material is available at:
http://www.serbiosoc.org.rs/NewUploads/Uploads/Kocovic%20et%20al_6211_Supplementary%20Material.pdf.